ELSEVIER

Biophysical Chemistry 89 (2001) 25–34

Biophysical Chemistry

www.elsevier.nl/locate/bpc

# Conformation transition kinetics of regenerated *Bombyx mori* silk fibroin membrane monitored by time-resolved FTIR spectroscopy

Xin Chen[a,b,1], Zhengzhong Shao[a], Nebojsa S. Marinkovic[b,c], Lisa M. Miller[d], Ping Zhou[a], Mark R. Chance[b,c,*]

[a] *Department of Macromolecular Science, Key Laboratory of Molecular Engineering of Polymers, Fudan University, 220 Handan Road, Shanghai, 200433, PR China*

[b] *Center for Synchrotron Biosciences, Albert Einstein College of Medicine, 1300 Morris Park Avenue, Bronx, NY 10461, USA*

[c] *Department of Physiology and Biophysics, Albert Einstein College of Medicine, 1300 Morris Park Avenue, Bronx, NY 10461, USA*

[d] *National Synchrotron Light Source, Brookhaven National Laboratory, Upton, NY 11973, USA*

Received 7 August 2000; received in revised form 25 September 2000; accepted 25 September 2000

**Abstract**

The ethanol-induced conformation transition of regenerated *Bombyx mori* silk fibroin membrane from a poorly defined to the well ordered state was monitored by time-resolved Fourier transform infrared spectroscopy (FTIR) for the first time. From the analysis of FTIR difference spectra, taken on time scales as short as 6 s and up to 1 h after addition of ethanol, intensity vs. time plots of an increasing band at 1618 $cm^{-1}$ were observed indicating formation of a β-sheet coincident with the loss of intensity of a band at 1668 $cm^{-1}$ indicating decreases of random coil and/or silk I structure. Both infrared markers were fitted with identical biphasic exponential decay functions, however, there was a clear burst phase occurring prior to the onset of the observed transitions. The conformation transition process is indicated to either proceed sequentially through (at least) two intermediate states that contain different levels of β-sheet structure or to have parallel pathways of initial β-sheet formation followed by a slower 'perfection' phase. The first observed process forms in a burst phase a few seconds after mixing (or even faster), prior to the collection of the first spectrum at 6 s. The second observed process occurs with a time constant of ~0.5 min, the intermediate present at this stage then continues with a time constant of 5.5 min completing the observed formation of the β-sheet. The conformation transition of this slower intermediate is not only indicated by an analysis of the kinetics of

* Corresponding author. Tel.: +1-718-430-4136; fax: +1-718-430-8587.

*E-mail addresses:* chenx@fudan.edu.cn (X. Chen), mrc@aecom.yu.edu (M.R. Chance).

[1] Tel.: +86-21-6564-2866; fax: +86-21-6564-0293.



PII: S0301-4622(00)00213-1

the random coil and β-sheet-specific bands discussed above, it roughly coincides with the appearance of an additional infrared marker at 1695 $cm^{-1}$, which may be a marker for β-sheet structure specific to the formation of the perfected structure. The conformation transition of this protein analyzed by infrared spectroscopy provides insight into a part of the fascinating process of cocoon formation in *B. mori*. 

*Keywords:* Time-resolved FTIR spectroscopy; Protein conformation transition; *Bombyx mori* silk fibroin; β-Sheet conformation

## 1. Introduction

One of the most interesting problems of protein chemistry concerns the pathways of conformation transitions of proteins, i.e. the transition of the polypeptide chain from an often poorly defined state to its unique three-dimensional structure. Although much progress has been made in understanding this process for small proteins, the conformation transitions of larger structures is still considered potentially complex [1]. In this paper we examined the conformation transition of *Bombyx mori* silk fibroin, where the conformation transition is initiated by rapid changes in solvent conditions. This investigation is carried out as a model for the fascinating process corresponding to the mechanism for the change in conformation as water-soluble *B. mori* silk fibroin in silk glands is spun into a solid cocoon fiber [2,3].

*B. mori* silk fibers consist primarily of two components, silk fibroin and sericin. The majority of silk fibroin is highly periodic with simple repeating sections broken by more complex regions containing amino acids with bulkier side chains. The highly repetitive sections are composed of glycine, alanine and serine (approx. 85% in total) in a rough 3:2:1 ratio [4,5], and the amino acid sequence can be roughly expressed as $[gly–ala–gly–ala–gly–ser]_n$ [5–9]. These three residues contain short side chains and permit close packing through the stacking of hydrogen-bonded β-sheets. Previous studies of the structure of *B. mori* silk fibroin have revealed two different structural models, termed silk I and silk II [5,10]. Silk II is understood to be the extended β-sheet and silk I has remained poorly understood [6,8]. Through it is well known that the metastable silk I is obtained by air-drying of the contents of the silk gland and is considerably different from that of spun silk fibroin (silk II) by X-ray powder diffraction, its structure has remained unclear and disputable for approximately 50 years [11].

It is well known that *B. mori* silk fibroin exhibits a number of conformational states, however, there is some controversy as to the exact mixture of states. For instance, Trabbic and Yager reported β-helix, disordered helix, β-sheet, β-turn and undefined conformations using quantitative Raman spectroscopy [12] while Lazo and Downing suggested the presence of β-turns and β-helix using circular dichroic (CD) spectra, nuclear magnetic resonance data and computer modeling [13]. However, it is generally accepted that *B. mori* silk fibroin has three major conformations in the solid state, which are random coil, silk I structure and β-sheet (or silk II structure) [14,15]. There are many studies on the *B. mori* silk fibroin structure and its conformation transitions using different methods. For example, Canetti et al. investigated the conformation of silk fibroin in water and in water–organic solvent mixture by CD and small-angle X-ray scattering (SAXS). They found a disordered structure in water and a β-sheet conformation in aqueous organic solvents [14]. Yoshimizu studied the silk fibroin membrane in swollen state by means of spin-label ESR, $^{13}C$-NMR and FTIR (attenuated total reflectance method) spectroscopies. The results showed the conformation transition from random coil to β-sheet conformation when the membrane was immersed in 80% aqueous methanol. According to the experimental results, they proposed a heterogeneous structure model of the swollen silk fibroin [16].

In our previous work, we used Raman spectroscopy to examine the mechanical denaturation process of silk fibroin. These data indicated that the undrawn silk fibroin is mainly in the random

coil structure with some helical conformation. When the samples were drawn up to the ratio $R = 4$ ($R = l_{drawn}/l_{initial}$, where $l$ is length), the β-sheet conformation formed [17]. These studies support the idea that aqueous solutions of *B. mori* silk fibroin show mainly random coil conformations and they may also contain some fraction of silk I structure [14,16–19].

The most common method to convert the *B. mori* silk fibroin from random coil and/or silk I conformation to β-sheet is to add low dielectric constant organic solvents, such as methanol, ethanol, or dioxane to the samples [14,16,18,20,21]. Other methods, such as mechanical treatment [17,20], changes in temperature [22] or blending with other polymers (like chitosan [23] and sodium alginate [24]) also can change the conformation of *B. mori* silk fibroin.

FTIR spectroscopy is a powerful method to examine protein structure as well as conformation transition processes. In particular, the amide I band can be deconvolved into discreet components indicative of random coil, α-helical, and β-sheet structures [25–28]. Time-resolved infrared spectroscopy on timescales as short as picoseconds have examined helical transitions and other folding processes [29–33]. In this paper, we used time-resolved infrared spectroscopy to investigate the ethanol-induced conformational transition processes of regenerated *B. mori* silk fibroin membrane. Because of the large molecular weight of *B. mori* silk fibroin (approx. 300 000–360 000 Da [34–38]), the conformation transition takes place on the minutes time scale, so that the time-resolved data can be easily obtained. The results suggest the presence of intermediates in the conformation transition during the progression of *B. mori* silk fibroin membrane from random coil and/or silk I structure to a β-sheet structure.

## 2. Materials and methods

### 2.1. Preparation of regenerated B. mori silk fibroin membrane

Raw silk consists of fibroin fibers that are bound together by several hydrophilic coat proteins, or sericins, and only the hydrophobic fibroin protein was examined in this study. Thus, the raw silk was degummed to remove the sericins. Degumming was accomplished by twice boiling the silk in 0.5% (w/w) $NaHCO_3$ solution for 30 min. The degummed fibers were then washed with copious amounts of distilled water and allowed to air dry at room temperature.

When making regenerated *B. mori* silk fibroin membranes, dry degummed silk fibers were dissolved in 9.5 mol/l LiBr aqueous solution according to established procedures [4,9,12,15,18,22,39]. After dialysis against pure water for 3 days, the solution was filtered. The concentration of the *B. mori* silk fibroin is approximately 1.0% (w/w). The *B. mori* silk fibroin solution was cast onto a polyethylene plate, then allowed to dry at approximately 25°C and 50% relative humidity. After several days, the regenerated *B. mori* silk fibroin membranes were obtained. The thickness of the membrane was approximately 5 μm.

### 2.2. FTIR measurement

All infrared spectra were recorded using a Nicolet Magna 860 FTIR spectrometer. To eliminate spectral contributions due to atmospheric water vapor, the instrument was continuously purged by nitrogen using the blow-off of a liquid nitrogen tank. The infrared spectra were recorded using a liquid nitrogen cooled MCT detector. For each measurement, 64 interferograms were coadded and Fourier-transformed employing a Genzel–Happ apodization function to yield spectra with a nominal resolution of 4 $cm^{-1}$.

The *B. mori* silk fibroin membranes were cut into discs with a diameter of 5 mm. For the time-resolved measurements, the *B. mori* silk fibroin membrane was placed between a pair of $BaF_2$ windows separated by a path length of 15 μm in a liquid cell. As soon as the 70% ethanol/30% $D_2O$ solution was injected into the cell, the measurements were started. Due to the parameter chosen above (64 scans per spectrum and the resolution of 4 $cm^{-1}$), the interval between two successive spectra in the *Rapid Scan*

mode is 0.0975 min. The total data collection time was 60 min in this measurement.

Absorbance spectra at each time point were generated by dividing the single beam spectrum collected at a specific time by a background spectrum and converting to absorbance using OMNIC 5.1 (Microcal). The difference spectra were calculated by the subtraction of an absorbance spectrum collected at time $t$ after addition of solvent from the first absorbance spectrum. The data shown in the figures are from a single experiment. For the kinetic results presented in the table, the results from three separate experiments were averaged and the reported errors represent the standard deviation of the measurements. Kinetic fitting was carried out using ORIGIN 5.0 (Microcal). No smoothing was used for the equilibrium or kinetic difference spectra, except nine-point smoothing was used prior to the taking of second derivatives.

Measurements under equilibrium conditions were also taken. In this case the *B. mori* silk fibroin membrane was examined without any treatment and the membrane was also examined after immersing in 70% ethanol/ 30% $D_2O$ solution for 24 h. For the latter measurements the membrane was dried after ethanol treatment and spectra were recorded using the normal scan mode.

## 3. Results and discussion

### *3.1. FTIR spectra of regenerated B. mori silk fibroin membranes under equilibrium conditions*

FTIR spectra of *B. mori* silk fibroin membranes as prepared and after immersion in ethanol were recorded. To characterize the structure of the polypeptide, we examined the FTIR spectra in the amide I region. In Fig. 1a, it can be seen that the amide I band in the *B. mori* silk fibroin membrane without any treatment is a broad, slightly asymmetric envelope with a center at around 1650–1660 $cm^{-1}$. Overall, these data are characteristic of random coil and/or silk I conformation [26,40]. By contrast, the spectrum of the amide I band of the silk fibroin membrane immersed into ethanol, Fig. 1b, is quite complex, with significant components around 1620 and 1695 $cm^{-1}$, while the fraction of absorbance around 1655–1660 $cm^{-1}$ is vastly reduced. In order to examine the multiple components in the amide I peak, second derivative techniques are used to examine the spectra. From the second derivative spectra in Fig. 1a, the peak around 1655–1660 $cm^{-1}$ accords with the original spectrum and the analysis did not reveal additional resolved subcomponents except a possible additional component at $\sim$1680 $cm^{-1}$, which becomes prominent upon additional smoothing of the derivative spectrum (not shown). In Fig. 1b, the second derivative analysis clearly reveals the two components at around 1620 and 1695 $cm^{-1}$, which are characteristic of the β-sheet conformation [15,16,23]. As in the original spectra, the peak attributed to random coil and/or silk I structure (1655–1660 $cm^{-1}$) is significantly diminished. The second derivative spectra clearly show that β-sheet structure is formed while random coil and silk I structure are decreased after ethanol treatment.

The first spectrum in the dynamic measurement (recorded at $\sim$0.1 min after the addition of ethanol) is shown in Fig. 1c. It indicates a significant amount of β-sheet structure was formed during a burst phase occurring prior to the first measurement. The second derivative reveals the same general components seen in Fig. 1b, however, a much greater amount of the random coil structure exists. Ideally, this burst phase can be easily obtained by calculating $(Abs_{Fig1c} - Abs_{Fig1a})/(Abs_{Fig1b} - Abs_{Fig1a})$. However, the silk fibroin samples for equilibrium and dynamic measurements have different thicknesses (though they were cut from same membrane), so that the absorbance spectra do not subtract well. This shortcoming is very difficult to overcome because *B. mori* silk membrane is very thin and brittle, and it is difficult to measure the thickness accurately. Moreover, the backgrounds of Fig. 1a,b (air) and Fig. 1c (70% ethanol/30% $D_2O$) are not the same, which makes for additional difficulties in the subtraction of spectra. Despite the difficulties, we found a feasible way to estimate the burst

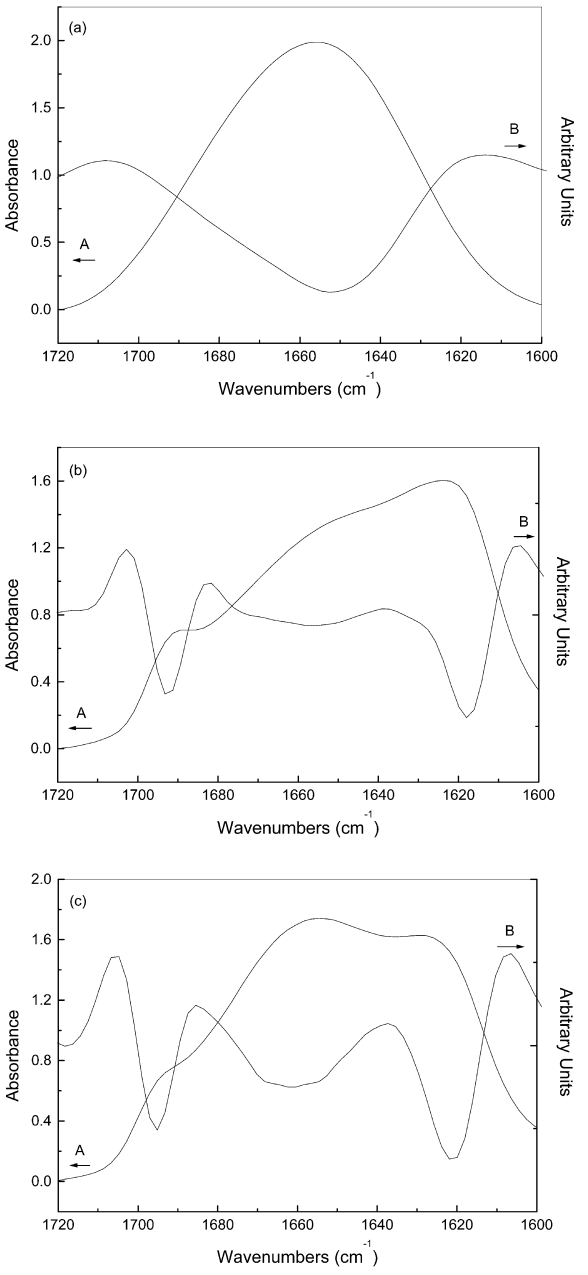


Fig. 1. Amide I band of regenerated *B. mori* silk fibroin: (a) membrane without any treatment; (b) membrane immersed in 70% ethanol for 24 h and then dried; (c) the first spectrum (at ~0.1 min) in the dynamic measurement (curve A: normal FTIR spectrum; curve B: second derivative spectrum).

phase as follows: the burst phase was estimated by calculating $(Abs_C - Abs_A)/[(Abs_B - Abs_C) + (Abs_C - Abs_A)]$ (where Abs denotes the absorbance spectrum). We first took the spectrum before the conformation transition ($Abs_A$), then injected ethanol–$D_2O$ mixture to allow the conformation transition to begin. From the series of dynamic spectra, we chose the last spectrum (~60 min) and the first spectrum (~0.1 min) to get $Abs_B$ and $Abs_C$. Using these spectra as a basis for calculation, we can ensure that the sample position had minimal changes during the measurement and also ensure the membrane thickness changes were minimal. Afterwards, using baseline corrections (to correct background differences), we subtracted $Abs_B - Abs_C$ (same background, small error) and $Abs_C - Abs_A$ (different background, larger relative error) to calculate the burst phase. This analysis indicates a burst phase of $50 \pm 10\%$.

### *3.2. Time-resolved FTIR spectra collected during the conformation transition process of regenerated B. mori silk fibroin membrane induced by ethanol*

Fig. 2 shows the infrared absorbance spectra of the regenerated *B. mori* silk fibroin membrane during the conformation transition after the addition of ethanol, from 0.1 to 60 min. With increasing time, characteristic changes in the absorbance spectra are seen, i.e. the amide I band gradually changes from ~1660 $cm^{-1}$ to ~1620 $cm^{-1}$. These time-resolved changes are emphasized in the difference spectra (Fig. 3) which have been calculated according to $A_t$–$A_0$, where $A_t$ are the absorbance spectra at a running time and $A_0$ is the first absorbance spectrum, i.e. the one recorded at 0.0975 min (Fig. 1c). Note that in the difference spectra, the main difference features are identical with those identified by the second derivative analysis in Fig. 1b,c. The increasing positive band at 1618 $cm^{-1}$ reflects the increasing β-sheet structure that develops with time after addition of ethanol. Correspondingly, the one

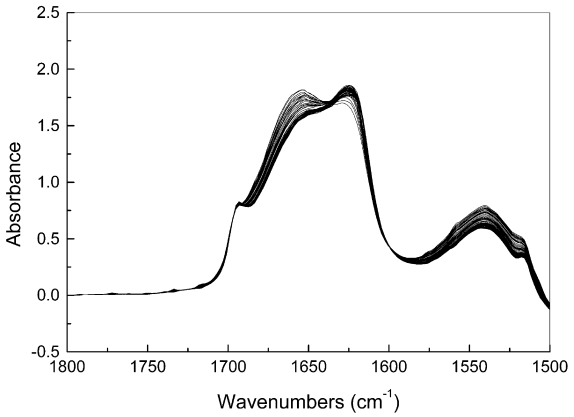


Fig. 2. Original FTIR spectra of regenerated *B. mori* silk fibroin membrane during the conformation transition process from beginning to 60 min.

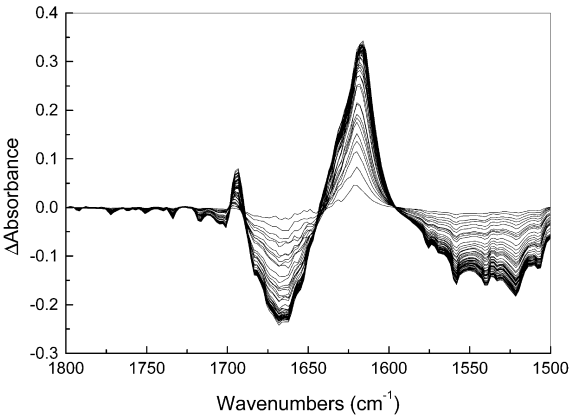


Fig. 3. Difference spectra obtained from Fig. 2.

negative band around 1668 $cm^{-1}$ indicates the loss of random coil and/or silk I structure during the process. In the meantime, a distinct positive band at 1693 $cm^{-1}$ (also indicating the formation of β-sheet structure) is observed.

### *3.3. Kinetics of the conformation transition and mechanism of folding of the regenerated B. mori silk fibroin membrane*

From the difference spectra, intensity–time plots can be generated for the kinetic measurements. Fig. 4a presents the results obtained employing the prominent difference band at 1618 $cm^{-1}$ as a probe for β-sheet conformation. The loss of random coil conformation represented by the decrease in the band at 1668 $cm^{-1}$ is plotted vs. time in Fig. 4b. The increasing curve in Fig. 4a and the decreasing curve in Fig. 4b appear coincident. The experimental data of both curves were fitted with biphasic exponential decay functions. The time constants and relative amplitudes for the fit to the increasing band at 1618 $cm^{-1}$ curve are identical to those observed for the decreasing curve representing the disappearance of random coil and/or silk I structure at 1668 $cm^{-1}$. These averaged results from three independent measurements are summarized in Table 1. The fitting procedure reveals two phases with time constants of $0.56 \pm 0.04$ min and $5.2 \pm 0.5$ min in the formation of β-sheet as well as two phases with time constants of $0.51 \pm 0.05$ min and $5.8 \pm 0.6$ min in the disappearance of random coil. The data analysis indicates that, within experimental error, the disappearance of random coil and/or silk I structure coincides with the appearance of the β-sheet

Table 1
Conformation transition kinetics of *B. mori* silk fibroin membranes probe by absorbance changes of β-sheet band at 1618 $cm^{-1}$ and random coil band at 1668 $cm^{-1}$ [a]

| IR 'marker' | $\tau_1$ (min) | $\alpha_1$ (%) | $\tau_2$ (min) | $\alpha_2$ (%) |
|---|---|---|---|---|
| β-sheet at 1618 $cm^{-1}$ | $0.56 \pm 0.04$ | $67 \pm 4$ | $5.20 \pm 0.47$ | $33 \pm 2$ |
| Random coil at 1668 $cm^{-1}$ | $0.51 \pm 0.05$ | $63 \pm 4$ | $5.80 \pm 0.61$ | $37 \pm 3$ |

[a] *Notes.* The time constants, τ, and the amplitudes were obtained by the absorbance difference spectral amplitudes with exponential decay functions. The relative amplitudes $\alpha_1$ and $\alpha_2$ were calculated by $\alpha_1 = A_1/(A_1 + A_2)$ and $\alpha_2 = A_2/(A_1 + A_2)$, respectively (where $A_1$ and $A_2$ are the amplitudes of the first and the second phase). All values represent the average of three measurements where the errors are 1 S.D.

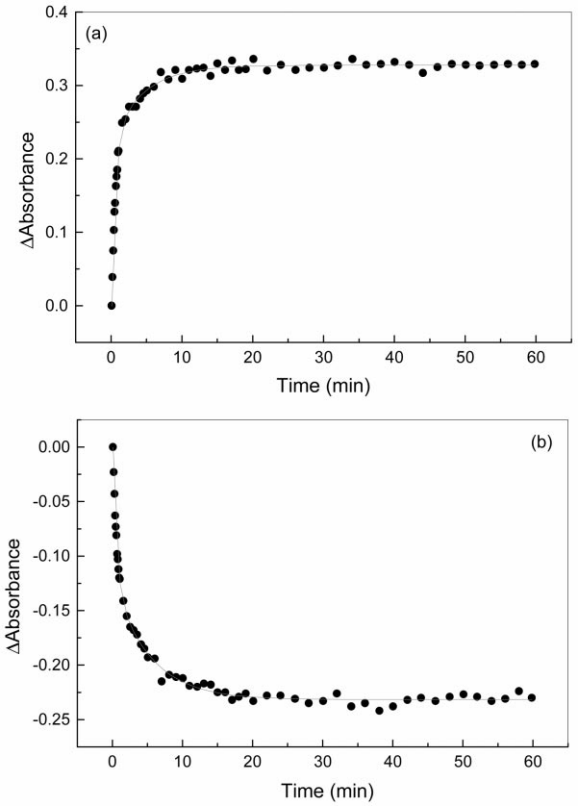


Fig. 4. Conformation transition kinetics of regenerated *B. mori* silk fibroin monitored by time-resolved FTIR spectroscopy: (a) increasing of β-sheet at 1618 $cm^{-1}$; (b) decreasing of random coil at 1668 $cm^{-1}$.

structure. In addition the amplitudes of two phases for both fits imply a ratio of 2:1 of the faster phase compared to the slower one.

Based on the observed data, we can establish which phases are sufficiently resolved in time to be kinetically distinguishable states. For example, the first spectrum at $\sim 0.1$ min indicates that $\sim 50\%$ of the protein has already attained β-sheet structure during the burst phase. The second process, with a time-constant of 0.5 min, constitutes $2/3$ of the measured reaction after the burst phase. Thus, this phase is 33% of the total folding reaction. We cannot determine from the data if the second process follows continuously from the burst phase or if there is a gap between the two phases.

At 5–6 min after addition of ethanol, the third process (representing $1/3$ of the folding after the burst phase) is one-half complete. However, by this time the second process has completed 10 half-times and is negligible. In addition, the reaction is examined out to an hour, so the third process is effectively fully completed (5–6 half-times). Thus, the third phase represents the transition process of a kinetically distinct species.

It is reasonable to suppose that the conformation transition of such a large fibrous protein is likely to be quite different than the conformation transition (folding) of small, cooperative proteins. For the small, cooperative proteins, the macroscopic properties observed are the sum of the behavior of each single protein molecule. However, the macroscopic properties (like mechanical properties) of a fibrous protein are highly related to its morphology and the intermolecular interactions of the individual protein segments. For instance, a single silk fibroin molecule obviously does not have any properties similar to the silk fibroin material (fiber, membrane, etc.). Therefore, the conformation transition process relates to the synergistic effects among numerous macromolecules. This suggests, a priori, at least two major phases to the conformation transition mechanism that includes the initial arrangement of individual protein segments and subsequently, the rearrangement of segments to complete the intermolecular interactions that result in a fiber with the appropriate macroscopic properties.

As stated above, we cannot determine whether the burst phase and the second process are kinetically distinct or continuous in nature. Also the possibility that parallel pathways exist must be considered in examining the conformation transition mechanism. For example the second process could represent a fraction of the population that is kinetically trapped. Such kinetic traps are a common feature of globular protein's conformation transition (folding) mechanisms, and can include partial misfolding of the protein structure as well a slowing down of the folding mechanism due to the need for *cis–trans* isomerization around prolyl peptide bonds [41]. The proline composition of *B. mori* silk fibroin is no more than 1% [6], but it is unclear at present what role, if any,

proline isomerization may play in the conformation transition mechanism.

### *3.4. Relative contributions of folding and assembly to the conformational dynamics observed*

The conformational rearrangements observed in this study are initiated when the silk fibroin membrane contacts the aqueous ethanol solution and the membrane swells. It is important to understand to what extent the infrared spectral changes represent the folding of individual protein segments vs. assembly of folded protein molecules into fibers. Because *B. mori* silk fibroin has a primary structure that is largely a regular alternation of glycine with alanine or serine, it has the intrinsic propensity to form a β-sheet structure under favorable conditions [14]. The initial state has a minimal β-sheet structure, despite this propensity to form β-sheet. This suggests that initially, the individual protein segments may be unfolded or partially folded. If so, then the burst phase representing 50% of the transition may reflect relatively fast folding of individual protein molecules to a more stable state. Subsequent to this burst phase, assembly of protein molecules into fibers, and the initiation of inter-molecular β-sheet formation may commence coincident with the second observed process having a time constant of $\sim 0.5$ min.

The conformation transitions of polymers prefer to occur in a mode that is kept local by distortion of nearby parts of the molecule and does not require gross movements of the macromolecule [42]. Thus, the silk fibroin molecules may form β-sheet structures by adjusting the individual protein segments first. Subsequent to this initial phase, the remaining segments may not be in favorable orientations to form additional β-sheet structures through intramolecular rearrangement. Therefore, the third observed process (with a time constant of 5.5 min) may include movement of whole macromolecular chains with respect to each other, a process required for the 'perfection' of the β-sheet structure formed initially in the faster phases.

This perfection process may also have multiple phases as indicated by the spectral data. Examination of the intensity–time plot also indicating β-sheet structure at 1693 $cm^{-1}$ from the difference spectra (Fig. 5) shows an initial lag phase in the kinetics followed by a slow change with a time constant of approximately 10 min. However, this kinetic behavior is very complex and does not fit a sum of exponentials or even a log–log analysis [43]. Clearly it does not coincide with the kinetics of the third phase measured above, and may be a separate structural change that is dependent on the formation of the product of the third phase.

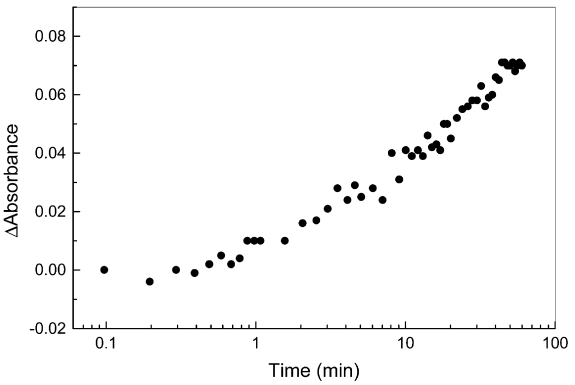


Fig. 5. The increasing of β-sheet at 1693 $cm^{-1}$ during the conformation transition process of regenerated *B. mori* silk fibroin membrane.

## 4. Conclusion

The kinetics of conformation transition of the *Bombyx mori* silk fibroin membrane from poorly defined to the well-ordered state was analyzed for the first time. Using FTIR spectroscopy, independent measures of the β-sheet conformation could be analyzed simultaneously with the loss of random coil structure. As would be expected for the molecular rearrangement of such a large protein system, the kinetics of formation of the 'perfected' state is slow, and multiple intermediate states are indicated. However, the initial formation of β-sheet structure, which accounts for 50% of the conformation transition mechanism, may be rapid. Further study is required to understand this interesting and complex conformation transi-

tion mechanism fundamental to the process of silk formation.

## Acknowledgements

The authors wish to thank Mr Michael Sullivan (Albert Einstein College of Medicine, Bronx, NY) for his valuable input into this collaborative project. This work is supported by Foundation for University Key Teacher by the Ministry of Education of China, the National Natural Science Foundation of China and by a grant from the National Center for Research Resources, National Institutes of Health, P41-RR-01633.

## References

[1] C.M. Dobson, A. Šali, M. Karplus, Protein folding: a perspective from theory and experiment, Angew. Chem. Int. Ed. 37 (1998) 868–893.

[2] K. Kerkam, C. Viney, D. Kaplan, S. Lombardi, Liquid crystallinity of natural silk secretions, Nature 349 (1991) 596–598.

[3] P.J. Willcox, S.P. Gido, W. Muller, D.L. Kaplan, Evidence of cholesteric liquid crystalline phase in natural silk spinning process, Macromolecules 29 (1996) 5106–5110.

[4] P. Monti, G. Freddi, A. Bertoluzza, N. Kasai, M.J. Tsukada, Raman spectroscopic studies of silk fibroin from *Bombyx mori*, J. Raman Spectrosc. 29 (1998) 297–304.

[5] Y. Shen, M.A. Johnson, D.C. Martin, Microstructural characterization of *Bombyx mori* silk fibers, Macromolecules 31 (1998) 8857–8864.

[6] B. Lotz, F. Colonna-Cesari, The chemical structure and crystalline structures of *Bombyx mori* silk fibroin, Biochime 61 (1979) 205–214.

[7] R. Valluzzi, S.P. Gido, The crystal structure of *Bombyx mori* silk fibroin at the air–water interface, Biopolymers 42 (1997) 705–717.

[8] T. Asakura, M. Demura, T. Date, N. Miyashita, K. Ogawa, M.P. Williamson, NMR study of silk I structure of *Bombyx mori* silk fibroin with $^{15}$N-and C-NMR chemical shift contour plots, Biopolymers 41 (1997) 193–203.

[9] M. Demura, M. Minami, T. Asakura, T.A. Cross, Structure of *Bombyx mori* silk fibroin based on solid state NMR orientational constraints and fiber diffraction unit cell parameters, J. Am. Chem. Soc. 120 (1998) 1300–1308.

[10] J. Magoshi, Y. Magoshi, S. Nakamura, in: D.L. Kaplan, W.W. Adams, B.L. Farmer, C. Viney (Eds.), Silk Polymers Materials Science and Biotechnology, American Chemical Society, Washington, DC, 1994, pp. 292–310.

[11] S.J. He, R. Valluzzi, S.P. Gido, Silk I structure in *Bombyx mori* silk foams, Int. J. Biol. Macromol. 24 (1999) 187–195.

[12] K.A. Trabbic, P. Yager, Comparative structural characterization of naturally and synthetically-spun fiber of *Bombyx mori* fibroin, Macromolecules 31 (1998) 462–471.

[13] N.D. Lazo, D.T. Downing, Stabilization of amphipathic α-helical and β-helical conformation in synthetic peptides in the presence and absence of ironic interactions, Macromolecules 32 (1999) 4700–4705.

[14] M. Canetti, A. Seves, F. Secundo, G. Vecchio, CD and small-angle X-ray scattering of silk fibroin in solution, Biopolymer 28 (1989) 1613–1624.

[15] T. Asakura, A. Kuzuhara, R. Tabeta, H. Saitô, Conformation characterization of *Bombyx mori* silk fibroin in the solid state by high-frequency $^{13}$C cross polarization-magic angle spinning NMR, X-ray diffraction, and infrared spectroscopy, Macromolecules 18 (1985) 1841–1845.

[16] H. Yoshimizu, T. Asakura, The structure of *Bombyx mori* silk fibroin membrane swollen by water studied with ESR, carbon-13 NMR and FTIR spectroscopies, J. Appl. Polym. Sci. 40 (1990) 1745–1756.

[17] S. Zheng, G. Li, W. Yao, T. Yu, Raman spectroscopic investigation of the denaturation process of silk fibroin, Appl. Spectrosc. 43 (1989) 1269–1272.

[18] M. Tsukada, Y. Gotoh, M. Nagura, N. Minoura, N. Kasai, G. Freddi, Physical and chemical properties of tussah silk fibroin films, J. Polym. Sci. Polym. Phys. 32 (1994) 961–968.

[19] G. Freddi, M. Romanò, M.R. Massafra, M. Tsukada, Structure and properties of tussah silk fibers graft-copolymerized with methacrylamide and 2-hydroxyethyl methacrylate, J. Appl. Polym. Sci. 56 (1995) 1537–1545.

[20] M. Ishida, T. Asakura, M. Yokoi, H. Saito, Solvent- and mechanical-treatment-induced conformational transition of silk fibroins studied by high-resolution solid-state $^{13}$C NMR spectroscopy, Macromolecules 23 (1990) 88–94.

[21] S.Y.U. Venyaminov, N.N. Kalnin, Quantiative IR spectrophotometry of peptide compounds in water ($H_2O$) solutions. II Amide absorption bands of polypeptides and fibrous proteins in A-,B-, and random coil conformations, Biopolymer 30 (1990) 1259–1271.

[22] C.X. Liang, K. Hirabayashi, Studies on mechanical properties of silk fibroin membranes, Polymer 33 (1992) 4388–4393.

[23] X. Chen, W. Li, T. Yu, Conformation transition on silk fibroin induced by blending chitosan, J. Polym. Sci. Polym. Phys. 35 (1997) 2293–2296.

[24] C.X. Liang, K. Hirabayashi, Mechanical properties of fibroin-chitasan membrane, J. Appl. Polym. Sci. 45 (1992) 1937–1943.

[25] P.I. Haris, D. Chapman, Microscopy, optical spectroscopy, and macroscopic techniques. studies on structure and stability of proteins using Fourier transform in-

frared spectroscopy, in: C. Jones, B. Mulloy, A.H. Tomas (Eds.), Methods in Molecular Biology, 22, Humana Press Inc, Totowa, NJ, 1994, pp. 183–202.
[26] W.K. Surewicz, H.H. Mantsch, New insight into protein secondary structure from resolution-enhanced infrared spectra, Biochim. Biophys. Acta 952 (1988) 115–130.
[27] A. Dong, P. Huang, W.S. Caughey, Protein secondary structures in water from second-derivative amide I infrared spectra, Biochemistry 29 (1990) 3303–3308.
[28] M. Sonoyama, M. Miyazawa, G. Katagiri, H. Ishida, Amplitude spectrum approach in dynamic FTIR spectroscopy, Appl. Spectrosc. 51 (1997) 545–547.
[29] D. Reinstädler, H. Fabian, J. Backmann, D. Naumann, Refolding of thermally and urea-denatured ribonuclease a monitored by time-resolved FTIR spectroscopy, Biochemistry 35 (1996) 15822–15830.
[30] C.M. Phillips, Y. Mizutani, R.M. Hochstrasser, Ultra-fast thermally-induced unfolding of Rnase A, Proc. Natl. Acad. Sci. USA 92 (1995) 7292–7296.
[31] J. Backmann, H. Fabian, D. Naumann, Temperature-jump induced RE-folding of ribonuclease A: a time-resolved FTIR spectroscopic study, FEBS Lett. 364 (1995) 175–178.
[32] S. William, T.P. Causgrove, R. Gilmanshin et al., Fast events in protein-folding: helix melting and formation in a small peptide, Biochemstry 35 (1996) 691–697.
[33] R. Gilmanshin, S. Williams, R.H. Callender, W.H. Woodruff, R.B. Dyer, Fast events in protein folding: relaxation dynamics and structure of the I form of apomyoglobin, Biochemistry 36 (1997) 15006–15012.
[34] E. Iizuka, J.T. Yang, The disordered and B. conformations of silk fibroin in solution, Biochemistry 7 (1968) 2218–2228.
[35] A.J. Hyde, C. Wippler, Molecular weight of silk fibroin, J. Polym. Sci. 58 (1962) 1083–1088.
[36] T. Sasaki, H. Noda, Studies on silk fibroin of *Bombyx mori* directly extracted from the silk gland I molecular weight determination in quanidine hydrochloride or urea solutions, Biochim. Biophys. Acta. 310 (1973) 76–90.
[37] T. Sasaki, H. Noda, Studies on silk fibroin of *Bombyx mori* directly extracted from the silk gland II effect of reduction of disulfide bonds and subunit structure, Biochim. Biophys. Acta. 310 (1973) 91–103.
[38] K.U. Sprague, The *Bombyx mori* silk proteins: characterization of large polypeptides, Biochemistry 14 (1975) 925–931.
[39] C.C. Chen, S. Riou, S.L. Hsu, Characterization of silk crystallization behavior on highly oriented substrates, Langmuir 12 (1996) 1035–1039.
[40] Z.H. Ayub, M. Arai, K. Hirabayashi, Mechanisms of gelation fibroin solution, Polymer 35 (1994) 2197–2200.
[41] R.L. Baldwin, The nature of protein folding pathways: the classical versus the new view, J. Biomol. NMR 5 (1995) 103–109.
[42] E. Helfand, Dynamic of conformational transitions in polymers, Science 226 (1984) 647–650.
[43] M. Chance, B. Campbell, R. Hoover, J. Friedman, Myoglobin recombination at low temperature, J. Biol. Chem. 262 (1987) 6959–6961.